Reaction $\bar{p}n \to \pi^-\pi^-\pi^+$ at incident momenta below 1 GeV/c

S. N. Tovey, K. R. Parker,* G. Chapman, J. De Roach,† E. Gold,‡ P. Kasper, P. A. King, A. G. Klein, L. J. Martin, G. C. Mason, G. I. Opat, and J. W. G. Wignall

School of Physics, University of Melbourne, Parkville, Victoria, Australia 3052

(Received 26 October 1977)

We have studied the reaction $\bar{p}d \to 3\pi p_s$ at a number of incident momenta between 0.40 and 0.92 GeV/c. A full partial-wave analysis of the 3π system is presented. The Dalitz-plot density distribution is compared with that observed in other experiments at higher and lower momenta.

I. INTRODUCTION

We have made a "complete" spin-parity analysis of the reaction

$$\bar{p}d \to \pi^-\pi^-\pi^+ p_s \tag{1a}$$

at incident antiproton momenta between 0.42 and 0.95 GeV/c. The partial-wave-analysis program developed at the University of Illinois by Ascoli and co-workers[1] has been slightly modified for this purpose. In the absence of information on helicities, the method utilizes all available kinematic information.

Several groups have published data and analyses of $\bar{N}N \to 3\pi$ annihilations at rest.[2-6] Such analyses are comparatively straightforward; the initial state is usually assumed to be an S wave (singlet only for $\bar{p}n$, singlet and triplet for $\bar{p}p$) and the final state may be described by two variables (i.e., Dalitz plot). Following the discovery of a "hole" in the Dalitz plot for $\bar{p}n \to 3\pi$,[2] analyses of that channel have been oriented towards Veneziano models[3,7] and a rising-phase-shifts resonance model.[4] The channel $\bar{p}p \to 3\pi$ has been studied[5,6] within the framework of an isobar or final-state-interaction approach. Bettini *et al.*,[8] have studied $\bar{p}n \to 3\pi$ between 1.0 and 1.6 GeV/c with the Veneziano model; they use the Dalitz-plot distribution plus the moments of the angular distributions. The present study is, as far as we are aware, the first to be published at nonzero momenta below 1 GeV/c.

Section II discusses data selection and Sec. III the Dalitz-plot distribution. A summary of the partial-wave method is given in Sec. IV and the results of our analysis are given in Sec. V.

II. DATA SELECTION

The present analysis is based on an exposure of the BNL 30-in. bubble chamber, filled with deuterium. A total of 150 000 photographs were taken in an antiproton beam at 10 incident momenta between 0.40 and 0.92 GeV/c.

The film was scanned for antiproton interactions producing three charged tracks, consistent with pions, either with or without a short, heavily ionizing, proton track (stub). Events with proton tracks longer than 5 cm were rejected. Part of the film was independently rescanned and the single-scan efficiency was calculated to be 83%. After measurement, data were processed using MLGEOM, a version of the Rutherford Laboratory geometry program, and GRIND, the CERN kinematics program.

A clean sample of 3π events was selected on the basis of fit probability. Events were required to fit reaction (1a), a four-constraint hypothesis, with a probability greater than 0.5%. Of the events so selected, 18% also fitted the hypothesis that an extra π^0 was present and 7% fitted hypotheses with $K\bar{K}$ production. Except for cases where the ionization of a charged secondary favored the $K\bar{K}$ hypothesis, all ambiguous events were retained in the 3π sample, which totaled 2038 events.

Considering reaction (1a) as a quasi-two-body reaction,

$$\bar{p}d \to (3\pi)^- p_s \ , \tag{1b}$$

then it may be kinematically defined by three variables. We chose s, t, and M (see Fig. 1), where s, t have their usual meaning and M is the mass of the 3π system. Figure 2(a) is a plot of s vs M for the selected data; all events occurred at very small values of $t' = t - t_{\min}$. The structure seen in the projection onto the s axis [Fig. 2(b)] is due to the nine beam momenta used in the experiment. The two broad bumps in the M distribution [Fig.

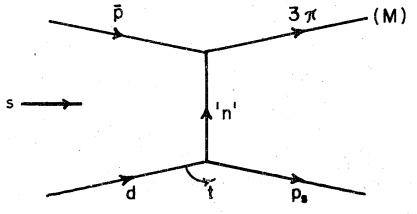

FIG. 1. Diagram for reaction (1b) illustrating the meaning of the kinematic variables used.

2(c)] are a manifestation of the relative amount of data of low- and high-beam momenta.

As will be discussed in the next section, the partial-wave analysis (PWA) program performs a fit

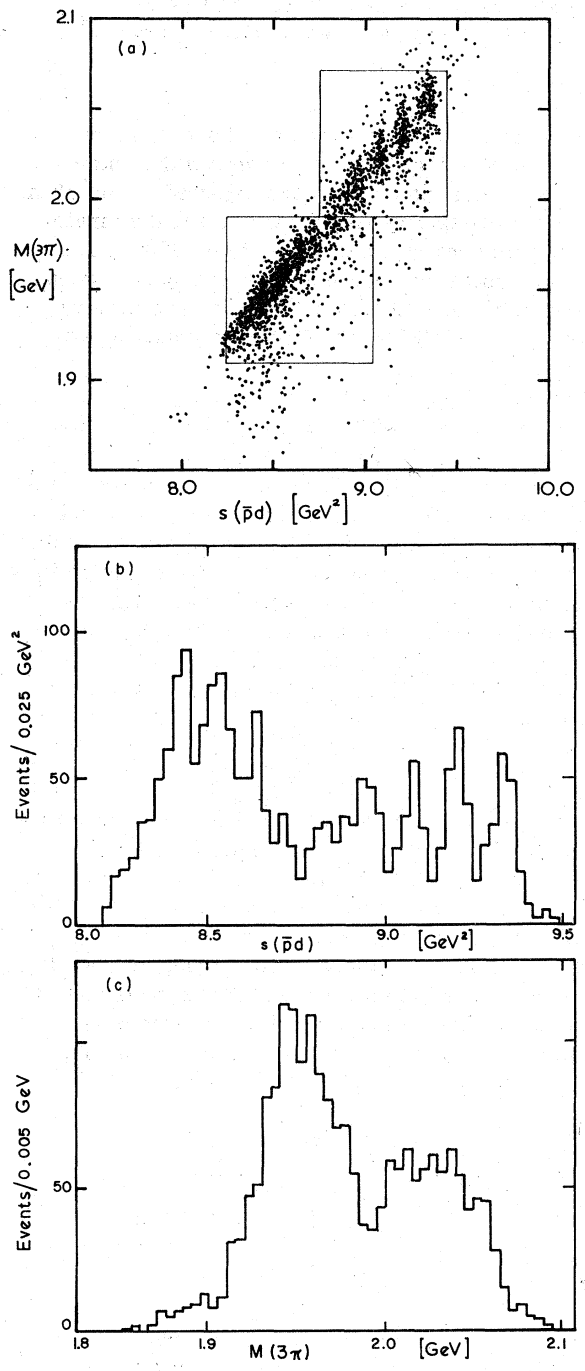

FIG. 2. (a) Scatter diagram of $M(3\pi)$ vs $s(\bar{p}d)$ for all events. The rectangles show the event samples selected for further analysis. (b) and (c) projection onto the $M(3\pi)$ and $s(\bar{p}d)$ axes.

TABLE I. Event samples used in the analysis.

Sample	A	B
M limits (GeV/c^2)	1.91–1.99	1.99–2.07
s limits (GeV^2)	8.24–9.04	8.74–9.44
t' limits (GeV^2)	<0.01	<0.01
No. of events	884	616

to the spin-parity states of the 3π system, averaged over intervals of s, M, and t (or t'). Since the program can only handle rectangles in the s-M plane, we define for the purpose of analysis the two data samples shown in Fig. 2(a). In addition, the cut $t' < 0.01$ GeV^2 is made. The two samples are defined in Table I.

In principle, five kinematic variables are needed to define the break up or decay of the three-meson system,

$$(3\pi)^- \to \pi_1^-\pi_2^-\pi_3^+ \ . \tag{1c}$$

We use the following set:

s_{13} and s_{23}, the invariant masses squared of the combinations $(\pi_1^-\pi_3^+)$ and $(\pi_2^-\pi_3^+)$.

ϕ, θ, and γ, three "Euler angles," defined in the $(3\pi)^-$ rest frame. ϕ and θ are, respectively, the azimuthal and zenith angles of the π^+ meson with respect to the axes $\hat{z} = \hat{p}(\bar{p})$, $\hat{y} = \hat{p}(p_s) \times \hat{z}$, $\hat{x} = \hat{y} \times \hat{z}$. γ is the azimuthal angle of π_1^- with respect to the axes $\hat{z}' = \hat{p}(\pi^+)$, $\hat{y}' = \hat{z} \times \hat{z}'$, $\hat{x}' = \hat{y}' \times \hat{z}'$. A further description of these angles may be found in Appendix B of Ref. 1.

The Dalitz plot for the 2038 selected events is given in Fig. 3. Figure 4 shows the distribution in

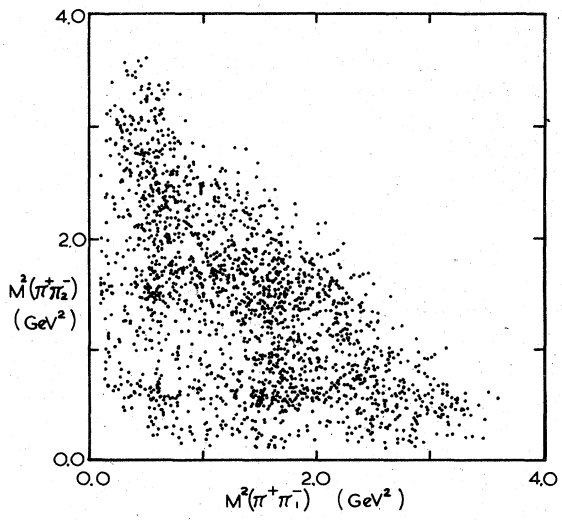

FIG. 3. The Dalitz plot for all accepted events.

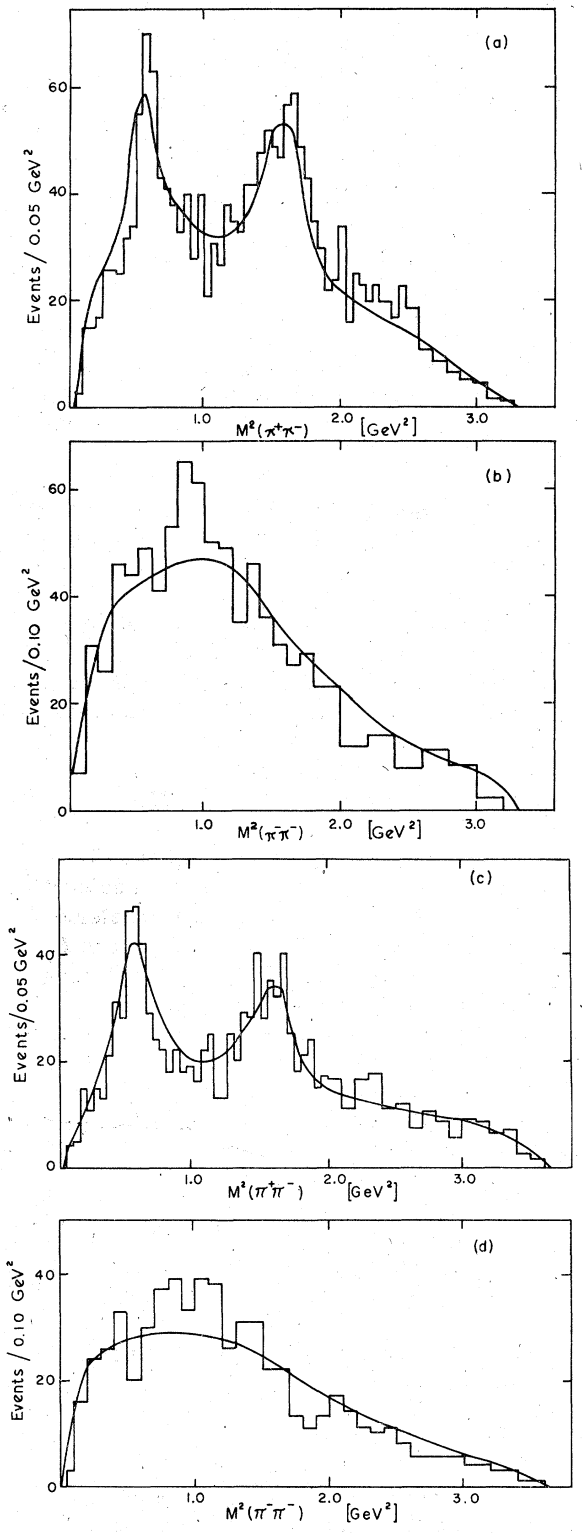

FIG. 4. Histograms of invariant mass squared for dipion combinations. (a) and (b) show $M^2(\pi^+\pi^-)$ and $M^2(\pi^-\pi^-)$ for event sample A, and (c) and (d) for sample B. The curves are the results of fits as discussed in the text.

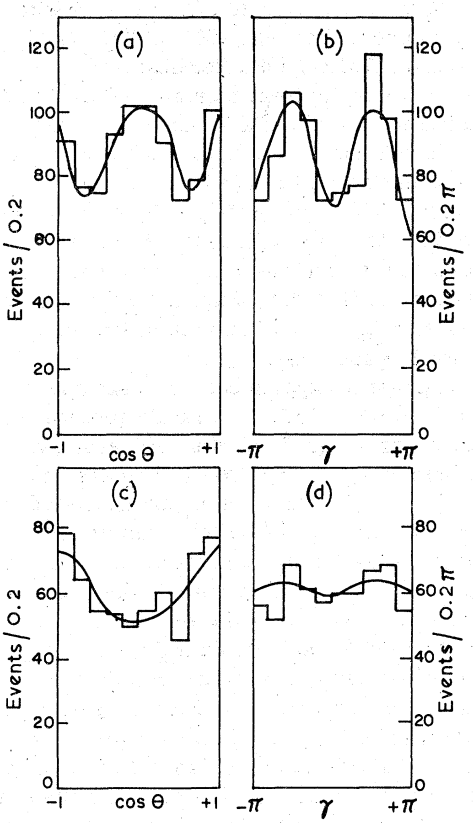

FIG. 5. Histograms of $\cos\theta$ and γ for the data. (a) and (b) refer to sample A, and (c) and (d) refer to B. The curves are the results of fits discussed in the text.

dipion masses for the events of samples A and B separately. These distributions are discussed in Sec. III.

The angle ϕ implies the existence of a production normal in the quasi-two-body reaction (1b). This requires that the direction of the recoiling proton stub (p_s) be well known. In about two-thirds of our data, p_s was unobserved and its direction was inferred from four-momentum balance. In the remaining one-third, p_s was observed but with a scanning bias. We therefore consider that the distribution in ϕ is likely to be biased. We remove this bias, together with any information carried by the ϕ distribution, by making a random rotation of the whole event about the beam direction ($\hat{z}$ axis). The experimental distributions in the other angles, $\cos\theta$ and γ, are given in Fig. 5.

III. THE DALITZ PLOT FOR $\bar{p}n \to \pi^-\pi^-\pi^+$

The first statistically significant experiment[2] on reaction (1a) at rest ($M \sim 1878$ MeV) revealed a striking absence of events (hole) near $s_{13} = s_{23} \approx 1$

GeV^2; however, a sample of 114 events with antiproton momenta between 100 and 300 MeV/c gave an isotropic Dalitz plot. Bettini *et al.*,[8] studying reaction (1a) at incident momenta above 1 GeV/c, found a similar hole at a 3π mass of $M \sim 2.15$ GeV. The hole was much less apparent when averaged over the interval $2.08 < M < 2.32$ GeV.

An early, although far from rigorous, explanation of the structure of the Dalitz plot was provided by Lovelace[7] within the Veneziano model. Odorico[9] has suggested that the "waxing and waning" of the hole of $s_{13} = s_{23} \approx 1$ GeV^2 may be produced by narrow s-channel resonances.

In the present experiment, the data span the region $1.9 < M < 2.1$ GeV. The Dalitz plot for all accepted events, Fig. 3, shows only weak evidence for a hole at $s_{13} = s_{23} \simeq 1$ GeV^2. The events occurring in that region have been carefully studied to ensure that they do not suffer from any pathology which would set them apart from the rest of the sample. The events occurring in the region of the putative hole were carefully examined by physicists, both on the scan table and post fitting. None of the events had a kinking track which might have biased its measurement, nor did they occur near the edge of the fiducial volume. The numbers of these events with an unseen spectator or with a competing kinematic fit were about as expected when compared to the complete sample. Finally, within the limited statistics, these events did not come from a particular range of beam momenta.

In conclusion, if a hole had not been previously observed in annihilations at rest and at 1.2 GeV/c, then any structure in the present Dalitz plot would have appeared to be quite consistent with resonance production corresponding to the ρ and f mesons.

IV. THEORY

The partial-wave analysis (PWA) program used here was written at the University of Illinois by Ascoli and co-workers. A detailed description of the method and its assumptions is to be found in Ref. 1. We restrict ourselves here to outlining the method and describing certain modifications that were necessary to analyze reaction (1a).

A. The "standard" version

The original program was written to study inelastic pion diffraction at high energies,

$$\pi^\pm p \to (3\pi)^\pm p' \quad . \tag{2}$$

Although the total energy is high, this reaction may be pictured, Fig. 6(a), as an annihilation of the incident π with an exchanged object (e.g., a Pomeron) at $M_{3\pi} \lesssim 2$ GeV. The 3π system of spin parity J^P, is considered to breakup or decay via a dipion

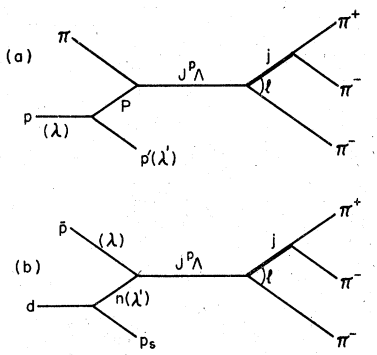

FIG. 6. A schematic diagram of angular momentum states in (a) $\pi p \to 3\pi p$ and (b) $\bar{p}d \to 3\pi p_s$.

resonance of spin j with angular momentum l relative to the third pion. The quantum numbers Λ^η also enter the analysis, Λ being the projection of J on the z axis ($|\Lambda| \leq J$) and η the eigenvalue of the reflection operator in the production plane. The amplitude for the reaction ($f_{\lambda\lambda'}$, where λ, λ' are the nucleon helicities) is expanded into partial waves with definite values of $J^P\Lambda^\eta lj$. The observed differential distribution is written

$$\omega(sMt;\, s_{13}s_{23},\, \phi\theta\gamma) = F + \sum_{ii'} M_i^* \rho_{ii'} M_{i'} \quad , \tag{3}$$

where i represents all quantum numbers $|i\rangle = |J^P\Lambda^\eta lj\rangle$, the kinematic variables are as defined in Sec. II, $M_i(s_{13}s_{23}\phi\theta\gamma)$ is a known matrix element, $\rho_{ii'}(sMt)$ is the unknown density matrix, and F stands for a "flat" or phase-space term (its significance is discussed below). The program fits, in each interval of (s, M, t), the elements $\rho_{ii'}$. In that no information on nucleon helicities is available, each $\rho_{ii'}$ is a bilinear combination arising from flip and nonflip terms and consequently the partial waves are incoherent in the sense that

$$|\rho_{ii'}| < (\rho_{ii}\rho_{i'i'})^{1/2} \quad .$$

The fit employs the maximum-likelihood method, utilizing all kinematic information, including correlations between variables. The results of the fit are the values of the complex density matrix elements ($\rho_{ii'}$). However, with a suitable normalization, the quantity

$$f_i = \rho_{ii} \int M_i^* M_i dx \quad , \tag{4}$$

where the integral dx extends over all of phase space, may be interpreted as the fraction of events associated with the state $|i\rangle$. Alternatively, a number of events may be quoted,

$$N_i = N f_i \quad , \tag{5}$$

where N is the total number of events in the sample.

The term F in the differential distribution, Eq. (3), represents an incoherent uniform phase-space distribution (hence "flat"). Ideally, such a term should not be needed as the partial-wave expansion is a complete description of the reaction amplitude. In practice, it is necessary to limit the expansion to low angular momentum values, to parametrize it, to average over extended kinematic regions, etc. The F contribution is intended to allow for these approximations to a complete partial-wave expansion; one expects that the number of associated events will be small.

B. The "modified" version

Reaction (1) may also be pictured [Fig. 6(b)] as an annihilation of the incident antiproton with neutron, slightly off the mass shell, leading to a three-pion system with mass ~2 GeV/c^2. The same partial-wave expansion may be made. Strictly, the amplitude now depends on the helicities of the $\bar{p}$, d, and p_s; in practice, in the spirit of the spectator model, the neutron can be considered as free and the amplitude depends on the helicities of the $\bar{p}$ (λ) and the n (λ').

A considerable simplification now occurs. The axis of quantization ($\hat{z}$) in the 3π rest frame is defined to be the common line of flight of the $\bar{p}$ and n. As a consequence, $\Lambda = \lambda - \lambda'$, and

(i) $\Lambda = 0$ states can be produced only when the helicities of the incident nucleons are equal. Therefore, all such states are coherent, i.e., $|\rho_{ii'}| = (\rho_{ii}\rho_{i'i'})^{1/2}$ if $\Lambda_i = \Lambda_{i'} = 0$,

(ii) $|\Lambda| = 1$ states arise when the incident helicities are opposite and, once again, are all coherently produced,

(iii) $\rho_{ii'} = 0$ if $\Lambda_i \neq \Lambda_{i'}$,

(iv) $|\Lambda| > 1$ states cannot be produced.

These conditions greatly reduce the number of parameters to be fitted. They also permit the unambiguous measurement, via the density matrix, of the various amplitudes and their phases.

The invariance of the reaction $\bar{p}n \to 3\pi$ under G parity places further restrictions on the permitted states. These restrictions are stronger than those normally derived from G parity in that they take into account the spin projection (Λ) of the system. The incident $\bar{p}n$ system has G parity $(-1)^{L+S+1}$, where L, S are the relative $\bar{p}n$ angular momenta and their total spin. The 3π final state has $G = -1$, and so we obtain the usual condition that

$$L + S = \text{even}\ .$$

In addition,

(i) $\Lambda = 0$ requires $\lambda = \lambda' = \pm\frac{1}{2}$,

$$G|J\Lambda, \lambda\lambda'\rangle = (-1)^{J+1}|J\Lambda, \lambda'\lambda\rangle = (-1)^{J+1}|J\Lambda, \lambda\lambda'\rangle,$$

therefore J = even ($0^-2^+2^-4^+4^-\ldots$);

(ii) $\Lambda = \pm 1$ requires $\lambda = -\lambda' = \pm\frac{1}{2}$, *and* $S = 1$, therefore L is odd, and $J^P = 1^+2^-3^+4^-\ldots$.

The absence of a production plane for our data (see Sec. II) means that η has no physical meaning and that equal populations are expected in the states $\Lambda^\eta = 1^+$ and 1^- (other quantum numbers being unchanged). This was observed within errors, and references to a $|J^P\Lambda = 1\rangle$ state in what follows implies a sum of $\Lambda = +1$ and $\Lambda = -1$ contributions.

Lastly, a word about errors. The PWA program assigns errors to the parameters ($\rho_{ii'}$) on the basis of the covariance matrix formed by the inverse of the matrix of the second differentials of the likelihood function with respect to these parameters.

V. ANALYSIS

A. Selection of resonant states

The limited number of events in each of our data samples and the large number of possible partial waves make some restrictions necessary. The dimeson state produced in the breakup of the 3π system is restricted to spin values $j = 0, 1, 2$. The states with $j = 1, 2$ were parametrized using Breit-Wigner amplitudes with masses and widths corresponding to the accepted values[10] for the ρ and f mesons. The $j = 0$ state (ϵ meson) was parametrized using the results of a $\pi\pi$ phase-shift analysis.[11] As will be discussed below, all states with $J \leq 4$ were considered, although not simultaneously. For each combination of J and j, only the lowest (or two lowest) allowed values of l were tried. Changing to an obvious spectroscopic notation [in which, for example, the state with $j = 1$, $l = 2$ is written $D(\rho\pi)$] we list in Table II the quantum numbers of the states used.

We first made a series of fits to test if certain states dominate reaction (1). The fits described below were made independently on each event sample. Reference to a state $|J^P\Lambda\rangle$ is understood to include all decays of that state, as listed in Table II. The density matrix at this stage was constrained to behave as predicted for a free-neutron target (see Sec. IV). That is,

All states with $\Lambda = 0$ (1) were assumed to be produced coherently.

No interference between $\Lambda = 0$ and $\Lambda = 1$ was permitted ($\rho_{ii'} = 0$ if $\Lambda_i \neq \Lambda_{i'}$). But see Sec. V(F) below.

TABLE II. Angular momentum states used in the analysis.

J^P	$j=0$ $(\epsilon\pi)$	$j=1$ $(\rho\pi)$	$j=2$ $(f\pi)$
0^-	S	P	D
1^+	P	S,D	P
2^-	D	P	S,D
3^+	F	D	P
4^-	G	F	D
1^-	...	P	D
2^+	...	D	P
3^-	...	F	D
4^+	...	G	F

Our procedure was as follows:

(1) To fit using all states with $J \leq 3$ which are consistent with G-parity conservation.

(2) Starting from fit (1) as a base, to try adding, one at a time, states with $J=4$ and states forbidden by G parity.

This procedure is similar to that commonly employed in other partial-wave analyses and, while obviously not completely satisfactory, is made necessary by the data sample available. It has the drawback that the number of events attributed to the particular decay of a definite $|J^P\Lambda\rangle$ state will fluctuate slightly depending on the presence in the fit of a quite separate state. However, the broad features of the fits presented below are stable with respect to the inclusion or not of additional marginal states.

B. The dominant $|J^P\Lambda\rangle$ states

In our first set of fits we included only those states with $J \leq 3$ which were allowed by G parity; there are six such states, plus the flat or phase-space term. These will be seen later to dominate the reaction. All decays of each state were included. The program had no difficulty in finding a "good" fit to each event sample (we consider later what is a good fit). The results of these fits are summarized in the next two tables.

Table III presents the percentages of events assigned to each $|J^P\Lambda\rangle$ state, summed over the decays of that state. The following points may be immediately remarked:

The $|J^P\Lambda\rangle = |0^-0\rangle$ state is strong and increases at higher masses.

The $|2^-0\rangle$ state, needed in the lower interval, has almost vanished at higher masses.

$J^P = 2^+$ waves are required but only in their $\Lambda = 0$ spin projection, $\Lambda = 1$ being insignificant.

The $|3^+1\rangle$ state, insignificant at low masses, is the dominant $\Lambda = 1$ state at high masses.

Bettini *et al.*,[8] in the interval $2.08 < M < 2.32$ GeV, find that the single Veneziano-type four-point function which best fits their data corresponds to $J^P = 2^+$. In our lower mass intervals, the $|J^P\Lambda\rangle = |2^+0\rangle$ state accounts for about 16% of the events.

We turn our attention now to the decay of these dominant $|J^P\Lambda\rangle$ states, as summarized in Table IV. For each event sample (A and B) we first included all the lowest-order decays (Table II) to to obtain fits A1 and B1. We then refitted excluding decays which were not required by the data (fits A2 and B2). In both samples this leads to a reduction of 18 in the number of parameters fitted. The corresponding reductions in the logarithmic likelihoods were 15 and 11 units, respectively, for samples A and B. This small ratio of likelihood reduction to parameter saving justifies the exclusion of these states. We may then see the following:

$|0^-0\rangle$ decays strongly into $S(\epsilon\pi)$. Owing to the large width of the ϵ meson, this decay looks very similar to phase space. A significant $D(f\pi)$ is seen but no $P(\rho\pi)$.

$|2^-0\rangle$ decays into many channels at low masses.

$|2^+0\rangle$ decays about equally into the two lowest-order-allowed channels $[D(\rho\pi)$ and $P(f\pi)]$.

At low masses $|1^+1\rangle$ is almost pure $P(\epsilon\pi)$. At higher masses some $\rho\pi$ is seen but as a D wave rather than an S wave.

$|3^+1\rangle$, strong only at higher masses, has as its dominant decay the $F(\epsilon\pi)$ channel.

From Table IV it is evident that, if we sum over spin-parity, then the final states $\epsilon\pi$, $\rho\pi$, $f\pi$, and phase space contribute about equally to sample A. At higher masses, sample B, this is still broadly true although $\epsilon\pi$ has gained somewhat at the expense of phase space.

It may be noticed that the percentages in each column of Table IV do not quite sum to 100%. This is because states with the same values of $|J^P\Lambda\rangle$ but different $|lj\rangle$ can interfere even after integra-

TABLE III. The percentages of events attributable to the $|J^P\Lambda\rangle$ states.

$J^P\Lambda$	Sample A; fit A1 low mass	Sample B; fit B1 high mass
0^-0	19.1±5.5	32.4±9.0
2^+0	16.2±2.7	15.2±3.3
2^-0	21.8±6.8	2.3±2.3
1^+1	16.5±5.9	9.0±4.5
2^+1	2.4±2.8	0.7±1.6
3^+1	3.2±3.7	26.7±4.7
"flat"	20.8±5.4	13.7±7.0

TABLE IV. The percentage of events attributable to the separate decays of the main $|J^P\Lambda\rangle$ states.

$\|J^P\Lambda; lj\rangle$	Sample A low mass Fit A1	Sample A low mass Fit A2	Sample B high mass Fit B1	Sample B high mass Fit B2
0^-0 $S(\epsilon\pi)$	9.8±4.8	8.9±3.3	24.4±8.0	23.6±6.5
$P(\rho\pi)$	0.9±1.4	•••	1.8±2.3	•••
$D(f\pi)$	7.2±2.4	7.9±2.4	5.2±3.1	7.0±2.9
2^-0 $D(\epsilon\pi)$	2.1±2.0	2.5±2.0	0.2±1.1	••◦
$P(\rho\pi)$	5.9±2.4	6.7±2.0	1.1±1.8	•••
$S(f\pi)$	5.0±1.9	5.7±1.8	0.2±0.5	•◦•
$D(f\pi)$	5.5±2.0	6.0±1.7	1.0±1.6	•◦◦
2^+0 $D(\rho\pi)$	10.5±3.0	11.4±2.6	8.9±3.6	8.5±3.4
$P(f\pi)$	9.9±2.8	9.5±2.7	11.4±4.1	12.3±3.7
1^+1 $P(\epsilon\pi)$	14.5±5.0	17.0±5.2	3.4±3.3	5.5±2.9
$S(\rho\pi)$	1.2±1.8	•••	0.3±0.8	••◦
$D(\rho\pi)$	0.1±0.6	•◦◦	3.1±2.1	3.4±2.0
$P(f\pi)$	0.0±0.2	•••	0.8±1.0	•••
2^+1 $D(\rho\pi)$	2.0±2.2	••◦	0.3±0.5	••◦
$P(f\pi)$	1.4±1.5	•••	1.1±1.4	••◦
3^+1 $F(\epsilon\pi)$	2.3±2.0	•••	15.3±3.6	16.2±3.9
$D(\rho\pi)$	1.2±1.1	◦••	4.5±1.8	5.0±2.0
$P(f\pi)$	0.2±0.6	◦••	6.5±2.1	7.0±1.9
"flat"	20.3±5.5	25.8±5.9	13.8±7.0	15.6±6.5

tion over all of phase space. (This is not true of states with different $|J^P\Lambda\rangle$ which can only interfere in the differential distribution.) As a result, the number of events attributed to a certain $|J^P\Lambda\rangle$ state is not in general the sum of the individual $|J^P\Lambda\rangle$ substates. In some cases large interference effects were observed, which will be discussed later.

C. $J=4$ and G-parity-violating states

We have searched for states with $J=4$ and for states forbidden by G parity. The statistical limitation of the data does not permit a simultaneous fit to all such states. We took, as a base, fits A2 and B2 which included the important decays of allowed states with $J\leq 3$. We made a series of fits, adding, one at a time, the new states. The results of these fits are given in Fig. 7.

The percentages of events attributed to the six $|J^P\Lambda\rangle$ states in the base fits were given in Table III and are repeated in Fig. 7. The percentages of events in the new ($J=4$ and G forbidden) states are also shown. Because of the way the fits were done, the percentages in Fig. 7 sum to a little more than 100%.

One may remark immediately that $J=4$ states are not required at these energies. This confirms the simple prediction that $J_{\max}\approx 3$ obtained from $J_{\max}=kR+1$, when k is the c.m. momentum and $R\approx 1$ fm is the interaction radius (see, for example, Montanet[12]). It also agrees with the observation of Carter *et al.*,[13] for the reaction

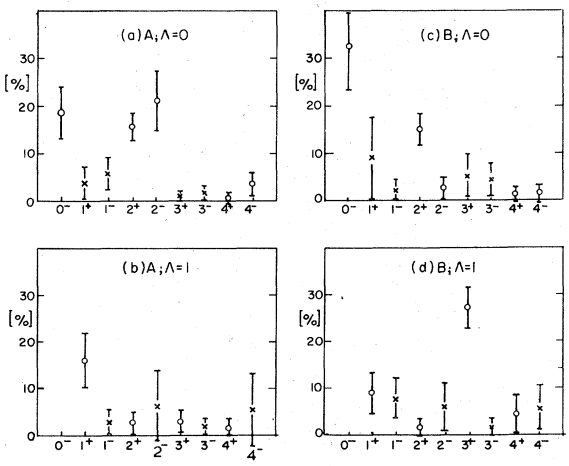

FIG. 7. The percentages of events fitted to various spin-parity states. (a) and (b) refer to sample A (low mass) with $\Lambda=0$ and 1, respectively; (c) and (d) refer to sample B (high mass) with $\Lambda=0$, 1. Open circles (○) refer to states allowed by G parity and crosses (×) to forbidden states.

$\bar{p}p \to \pi^+\pi^-$, where states with $J \geq 4$ are found to be insignificant at laboratory momenta below 1.0 GeV/c.

G-parity forbidden states are clearly suppressed. (The nature of the fitting program requires that the number of events in any state be non-negative.) In the low-mass data with $\Lambda = 0$, the forbidden $J = 1$ states are much lower than the allowed $J = 0, 2$ states. In the high-mass data the $J^P = 3^+$ state is present in its allowed $\Lambda = 1$ projection and is consistent with zero in its forbidden $\Lambda = 0$ projection. In other places, the results are less statistically convincing but no G-parity–forbidden state is seen at more than 1.5 standard deviation as compared to the seven allowed states.

D. Search for resonant behavior

In order to be able to assert that a state is resonant, the number of events should be seen to pass through a maximum, and preferably the relative phase of the state should be seen to exhibit the expected change. These effects are clearly impossible to observe with only two mass intervals. In order to search for resonant behavior we divided our data into five smaller samples. Each sample was fitted with the same set of waves, namely all those required either in fit A2 or in fit B2. Within our statistical precision, no resonant behavior could be seen.

E. Goodness of fit

A general feature of maximum-likelihood analyses is that they provide a "best fit" without any indication that it is a good fit. We generated large numbers of Monte Carlo events corresponding to fits A2 and B2. These Monte Carlo data, normalized to the numbers of events, are shown superimposed on the real data in Figs. 4 and 5. The general agreement is good. In both samples, a small excess of events may be seen in $M^2(\pi^-\pi^-)$ close to 1 GeV^2. We conclude that fits A2 and B2 provide good descriptions of the data with a minimal number of partial waves.

Both of the final fits, A2 and B2, require 20 real parameters to describe the density matrix. This is many more than for $\bar{p}n \to 3\pi$ at rest (four for the Veneziano model[3] and 14 for the phase-shift resonance model[4]). But it should be remembered that, at rest, only one spin-parity state ($J^P = 0^-$) contributes, while here we must consider at least six states (see Table III).

F. Test of the spectator hypothesis

In all of the fits made above, the density matrix was constrained such that $\rho_{ii'} = 0$ if $\Lambda_i \neq \Lambda_{i'}$. This requirement would be exactly satisfied for a free-neutron target.

We refitted the data, in samples A and B, starting with the results of fits A2 and B2, but allowing $\rho_{ii'}$ to be nonzero. The fitted values obtained were quite consistent with zero, indicating that the spectator hypothesis is valid.

G. Relative phases

The off-diagonal elements of the density matrix are complex numbers. Since all states with $\Lambda = 0$ (or $\Lambda = 1$) are produced coherently, see Sec. IV, the argument of this matrix element ($\rho_{ii'}$) is the phase difference between the amplitudes ($h_i, h_{i'}$),

$$\rho_{ii'} \propto h_i h_{i'}^*,$$

$$\mathrm{Arg}\,\rho_{ii'} = \phi_i - \phi_{i'}.$$

Thus, in principle we may determine relative phases. In practice when the number of events associated with a given state is small, then the errors on the phase differences become very large. However, we can measure the phases between the decays of the dominant states. It should be noted that for $\Lambda = 0$, parity conservation implies that the natural (2^+) and unnatural ($0^-, 2^-$) spin-parity series cannot interfere, and so no information on phases between these groups of states is possible.

Our results may be seen in Fig. 8. They are taken from fits A1 and B1 discussed earlier. For each of the three groups of states ($0^-, 2^-$ with $\Lambda = 0$, 2^+ with $\Lambda = 0$, $\Lambda = 1$) we must arbitrarily fix one phase. For the sake of clarity, we have only shown those states for which the relative phase was determined to within ±40°. Each state is shown as a vector in the complex plane, the length of each vector being proportional to the square root of the fraction of events in that state (Table IV). The following conclusions may be drawn, in spite of the large errors:

(i) $\Lambda = 0$, $J^P = 0^-, 2^-$. We fix the most important partial wave, $0^-S(\epsilon\pi)$, on the positive real axis. In both mass intervals the $D(f\pi)$ decay of the $J^P = 0^-$ is close to the negative real axis. At lower masses, all the decays of $J^P = 2^-$ are grouped near the negative imaginary axis. At higher masses, 2^- states are greatly diminshed but the only well-determined phase, for $2^-D(f\pi)$, puts that state near the negative imaginary axis also.

(ii) $|J^P\Lambda\rangle = |2^+0\rangle$. In both mass intervals the relative phase between $D(\rho\pi)$ and $P(f\pi)$ is about −45°. This leads to strong destructive interference. Averaging over the two mass intervals, the approximate numbers of events due to $\rho\pi$, $f\pi$, ρ-f interference are in the ratios 1, 1, $-\frac{1}{2}$.

(iii) $\Lambda = 1$. The dominance of different states in each mass interval (1^+ and 3^+, respectively) makes it hard to make any meaningful statements here.

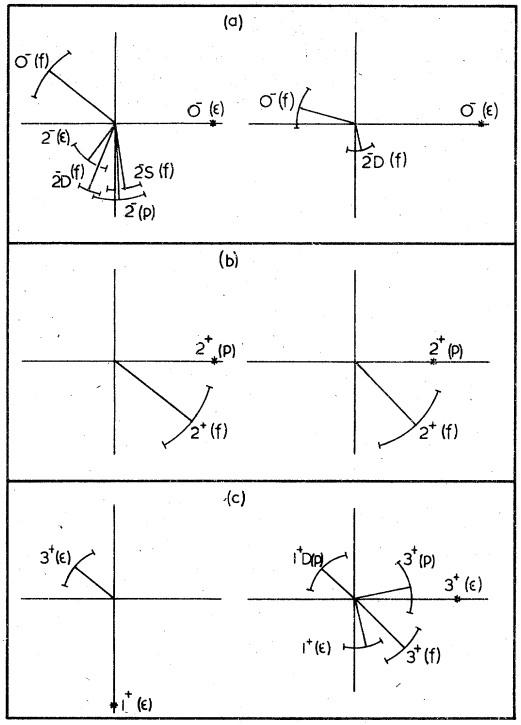

FIG. 8. Amplitudes in the complex plane, see text for details. The left-hand column refers to low-mass data (fit A1), the right-hand column to high-mass data (fit B1). (a) states with $\Lambda=0$, $J^P=0^-$, 2^- (b) $\Lambda=0$, $J^P=2^+$ (c) $\Lambda=1$. States marked with an asterisk had their phases arbitrarily fixed.

VI. SUMMARY AND CONCLUSIONS

We have demonstrated the feasibility of making partial-wave analyses of three meson states in nucleon-antinucleon annihilation. Even at the relatively modest energies of this experiment (0.40 to 0.92 GeV/c), many spin-parity states are found to contribute, and each of these states is observed to decay via several dimeson intermediate states. Data at least an order of magnitude better than that currently available are clearly desirable; however, one may already draw certain conclusions. For two intervals of 3π mass, from 1.91 to 1.99 and 1.99 to 2.07 GeV, we find the following:

(1) States with total angular momentum $J \geq 4$ are not required.

(2) All $|J^P\Lambda\rangle$ states forbidden by G-parity invariance are suppressed.

(3) $J^P=0^-$ pionlike states make important contributions in both mass intervals.

(4) The same conclusion holds for $J^P=2^+$ but only for spin projection $\Lambda=0$ (same helicities for incident $\bar{p}$ and n); the $\Lambda=1$ state (opposite helicities) is hardly required.

(5) The contribution from $|J^P\Lambda\rangle = |2^-0\rangle$ decreases between the mass intervals analyzed while that for $|3^+1\rangle$ increases sharply.

(6) In the breakup of the 3π system, roughly equal $\epsilon\pi$, $\rho\pi$, and $f\pi$ contributions are found.

(7) Those phases that we are able to measure are consistent between the two samples; we know of no model to predict these.

ACKNOWLEDGMENTS

We conclude by thanking the Brookhaven National Laboratory for the use of its facilities, our scanning and measuring staff for their careful work, and the Australian Research Grants Committee for financial support. Several of us (K.R.P., G.C., J.D.R., E.G., P.A.K., and L.J.M.) acknowledge the receipt of a Commonwealth Postgraduate Research Award.

*Present address: Department of Theoretical Physics, Oxford University.

†Present address: Central Research Laboratory, ICI, Ascot Vale, Melbourne, Australia.

‡Present address: Department of Applied Physics, Royal Melbourne Institute of Technology.

[1]J. D. Hansen, G. T. Jones, G. Otter, and G. Rudolph, Nucl. Phys. B81, 403 (1974); see also G. Ascoli *et al.*, Phys. Rev. Lett. 25, 962 (1970); G. Ascoli *et al.*, Phys. Rev. D 7, 669 (1973).

[2]P. Anninos, L. Gray, P. Hagerty, T. Kalogeropoulos, S. Zenone, R. Bizzarri, M. Gaspero, I. Laakso, S. Lichtman, and G. C. Moneti, Phys. Rev. Lett. 20, 402 (1968).

[3]G. P. Gopal, R. Migneron, and A. Rothery, Phys. Rev. D 3, 2262 (1971); 4, 2169 (1971).

[4]A. M. Gleeson, W. J. Meggs, and M. Parkinson, Phys. Rev. Lett. 25, 74 (1970).

[5]S. U. Chung, L. Montanet, S. Reucroft, and O. Witt-Hansen, Nucl. Phys. B31, 261 (1971).

[6]C. Baltay, P. Franzini, N. Gelfand, G. Lutjens, J. Severiens, J. Steinberger, D. Tycko, and D. Zanello, Phys. Rev. 140, B1039 (1965).

[7]C. Lovelace, Phys. Lett. 28B, 264 (1968); G. Altarelli and H. Rubinstein, Phys. Rev. 183, 1469 (1969); S. Pokorski, R. O. Raitio, and G. H. Thomas, Nuovo Cimento 7A, 828 (1972); R. Jengo and E. Remiddi, Lett. Nuovo Cimento 1, 637 (1969).

[8]A. Bettini, M. Cresti, M. Mazzucato, L. Peruzzo, S. Sartori, G. Zumerle, M. Alston-Garnjost, R. Huesman, R. Ross, F. T. Solmitz, L. Bertanza, R. Carrara, R. Casali, P. Lariccia, R. Pazzi, G. Boreani, B. Quassiati, G. Rinaudo, M. Vigone, and A. Werbrouck, Nuovo Cimento 1A, 333 (1971).

[9]R. Odorico, Phys. Lett. 33B, 489 (1970).

[10]Particle Data Group, Rev. Mod. Phys. 48, S21 (1976).

[11]S. D. Protopopescu *et al.*, in *Experimental Meson Spectroscopy—1972*, proceedings of the Third Inter-

national Conference, Philadelphia, edited by A. H. Rosenfeld and K.-W. Lai (AIP, New York, 1972), p. 17; G. Grayer *et al.*, *ibid.*, p. 5.
[12]L. Montanet, in *Proceedings of the Fifth International Conference on Elementary Particles, Lund, 1969,* edited by G. von Dardel (Berlingska Boktryckeriet, Lund, Sweden, 1970), p. 212.
[13]A. A. Carter, M. Coupland, E. Eisenhandler, W. R. Gibson, P. I. P. Kalmus, D. P. Kimber, A. Astburg, and D. P. Jones, Phys. Lett. 67B, 117 (1977).